The black hole bomb and superradiant instabilities

Vitor Cardoso*
Centro de Física Computacional, Universidade de Coimbra, P-3004-516 Coimbra, Portugal

Óscar J. C. Dias†
Centro Multidisciplinar de Astrofísica - CENTRA, Departamento de Física,
F.C.T., Universidade do Algarve, Campus de Gambelas, 8005-139 Faro, Portugal

José P. S. Lemos‡
Centro Multidisciplinar de Astrofísica - CENTRA, Departamento de Física,
Instituto Superior Técnico, Av. Rovisco Pais 1, 1049-001 Lisboa, Portugal

Shijun Yoshida§
Centro Multidisciplinar de Astrofísica - CENTRA,
Departamento de Física, Instituto Superior Técnico,
Av. Rovisco Pais 1, 1049-001 Lisboa, Portugal ¶
(Dated: February 1, 2008)

A wave impinging on a Kerr black hole can be amplified as it scatters off the hole if certain conditions are satisfied giving rise to superradiant scattering. By placing a mirror around the black hole one can make the system unstable. This is the black hole bomb of Press and Teukolsky. We investigate in detail this process and compute the growing timescales and oscillation frequencies as a function of the mirror's location. It is found that in order for the system black hole plus mirror to become unstable there is a minimum distance at which the mirror must be located. We also give an explicit example showing that such a bomb can be built. In addition, our arguments enable us to justify why large Kerr-AdS black holes are stable and small Kerr-AdS black holes should be unstable.

PACS numbers: 04.70.-s

I. INTRODUCTION

Superradiant scattering is known in quantum systems for a long time, after the problems raised by Klein's paradox [1, 2]. However, for classical systems superradiant scattering was considered only much later in a paper by Zel'dovich [3] where it was examined what happens when scalar waves hit a rotating cylindrical absorbing object. Considering a wave of the form $e^{-i\omega t + im\phi}$ incident upon such a rotating object, one concludes that if the frequency ω of the incident wave satisfies $\omega < m\Omega$, where Ω is the angular velocity of the body, then the scattered wave is amplified. It was also anticipated in [3] that by surrounding the rotating cylinder by a mirror one could make the system unstable.

A Kerr black hole is one of the most interesting rotating objects for superradiant phenomena, where the condition $\omega < m\Omega$ also leads to superradiant scattering, with Ω being now the angular velocity of the black hole [4, 5, 6]. Feeding back the amplified scattered wave,

one can extract as much rotational energy as one likes from the black hole. Indeed, if one surrounds the black hole by a reflecting mirror, the wave will bounce back and forth between the mirror and the black hole amplifying itself each time. Then the total extracted energy should grow exponentially until finally the radiation pressure destroys the mirror. This is Press and Teukolsky's black hole bomb [7]. Nature sometimes provides its own mirror. For example, if one considers a massive scalar field with mass μ scattering off a Kerr black hole, then for $\omega < \mu$ the mass μ effectively works as a mirror [8, 9].

Here we investigate in detail the black hole bomb by using a scalar field model. Specifically, the black hole bomb consists of a Kerr black hole surrounded by a mirror placed at a constant r, $r = r_0$, where r is the Boyer-Lindquist radial coordinate. We study the oscillation frequencies and growing timescales as a function of the mirror's location, and as a function of the black hole rotation. A spacetime with a "mirror" naturally incorporated in it is anti-de Sitter (AdS) spacetime, which has attracted a great deal of attention recently. It could therefore be expected that Kerr-AdS black holes would be unstable. Fortunately, Hawking and Reall [10] have given a simple argument showing that, at least large Kerr-AdS black holes are stable. As we shall show, this is basically because superradiant modes are not excited for these black holes. Furthermore, we suggest it is not only possible but in fact highly likely that small Kerr-AdS black holes are unstable.

¶Present address: Science and Engineering, Waseda University, Okubo, Shinjuku, Tokyo 169-8555, Japan
*Electronic address: vcardoso@teor.fis.uc.pt
†Electronic address: odias@ualg.pt
‡Electronic address: lemos@kelvin.ist.utl.pt
§Electronic address: shijun@waseda.jp

II.   THE BLACK HOLE BOMB

A.   Formulation of the problem and basic equations

We shall consider a massless scalar field in the vicinity of a Kerr black hole, with an exterior geometry described by the line element:

$$ds^2 = -\left(1 - \frac{2Mr}{\rho^2}\right) dt^2 - \frac{2Mra\sin^2\theta}{\rho^2} 2dtd\phi + \frac{\rho^2}{\Delta} dr^2$$
$$+\rho^2 d\theta^2 + \left(r^2 + a^2 + \frac{2Mra^2\sin^2\theta}{\rho^2}\right) \sin^2\theta \, d\phi^2 \,,$$
(1)

with

$$\Delta = r^2 + a^2 - 2Mr \,, \qquad \rho^2 = r^2 + a^2\cos^2\theta \,. \quad (2)$$

This metric describes the gravitational field of the Kerr black hole, with mass M, angular momentum $J = Ma$, and has an event horizon at $r = r_+ = M + \sqrt{M^2 - a^2}$. A characteristic and important parameter of a Kerr black hole is the angular velocity of its event horizon Ω given by

$$\Omega = \frac{a}{2Mr_+} \,. \quad (3)$$

In absence of sources, which we consider to be our case, the evolution of the scalar field is dictated by the Klein-Gordon equation in curved spacetime, $\nabla_\mu \nabla^\mu \Phi = 0$. To make the whole problem more tractable, it is convenient to separate the field as [11]

$$\Phi(t,r,\theta,\phi) = e^{-i\omega t + im\phi} S_l^m(\theta) R(r) \,, \quad (4)$$

where $S_l^m(\theta)$ are spheroidal angular functions, and the azimuthal number m takes on integer (positive or negative) values. For our purposes, it is enough to consider positive ω's in (4) [4]. Inserting this in Klein-Gordon equation, we get the following angular and radial wave equations for $R(r)$ and $S_l^m(\theta)$:

$$\frac{1}{\sin\theta}\partial_\theta\left(\sin\theta\partial_\theta S_l^m\right)$$
$$+ \left[a^2\omega^2\cos^2\theta - \frac{m^2}{\sin^2\theta} + A_{lm}\right]S_l^m = 0, \quad (5)$$
$$\Delta\partial_r\left(\Delta\partial_r R\right) + \left[\omega^2(r^2+a^2)^2 - 2Mam\omega r + a^2m^2\right.$$
$$\left. -\Delta(a^2\omega^2 + A_{lm})\right]R = 0, \quad (6)$$

where A_{lm} is the separation constant that allows the split of the wave equation, and is found as an eigenvalue of (5). For small $a\omega$, the regime we shall be interested on in the next subsection, one has [5, 12]

$$A_{lm} = l(l+1) + \mathcal{O}(a^2\omega^2) \,. \quad (7)$$

Near the boundaries of interest, which are the horizon, $r = r_+$, and spatial infinity, $r = \infty$, the scalar field as

given by (4) behaves as

$$\Phi \sim \frac{e^{-i\omega t}}{r}e^{\pm i\omega r_*} \,, \quad r \to \infty \quad (8)$$
$$\Phi \sim e^{-i\omega t}e^{\pm i(\omega - m\Omega)r_*} \,, \quad r \to r_+ \,, \quad (9)$$

where the tortoise r_* coordinate is defined implicitly by $\frac{dr_*}{dr} = \frac{r^2+a^2}{\Delta}$. Requiring ingoing waves at the horizon, which is the physically acceptable solution, one must impose a negative group velocity $v_{\rm gr}$ for the wave packet. Thus, we choose $\Phi \sim e^{-i\omega t}e^{-i(\omega - m\Omega)r_*}$. However, notice that if

$$\omega < m\Omega \,, \quad (10)$$

the phase velocity $-\frac{\omega - m\Omega}{\omega}$ will be positive. Thus, in this superradiance regime, waves appear as outgoing to an inertial observer at spatial infinity, and energy is in fact being extracted. Notice that, since we are working with positive ω, superradiance will occur only for positive m, i.e., for waves that are co-rotating with the black hole. This follows from the time and angular dependence of the wave function, $\Phi \sim e^{i(-\omega t + m\phi)}$. The phase velocity along the angle ϕ is then $v_\phi = \frac{\omega}{m}$, which for $\omega > 0$ and $m > 0$ is positive, i.e., is in the same sense as the angular velocity of the black hole.

Here we shall consider a Kerr black hole surrounded by a mirror placed at a constant Boyer-Lindquist radial r coordinate with a radius r_0, so that the scalar field will be required to vanish at the mirror's location, i.e., $\Phi(r = r_0) = 0$. With these two boundary conditions, ingoing waves at the horizon and a vanishing field at the mirror, the problem is transformed into an eigenvalue equation for ω.

The frequencies satisfying both boundary conditions will be called Boxed Quasi-Normal frequencies (BQN frequencies, ω_{BQN}) and the associated modes will accordingly be termed Boxed Quasi-Normal Modes (BQNMs). The quasi stems from the fact that they are not stationary modes, and that BQN frequencies are not real numbers. Instead they are complex quantities, describing the decaying or amplification of the field. One expects that for a mirror located at large distances, or for small black holes, the imaginary part of the BQNs will be negligibly small and thus the modes will be stationary, corresponding to the pure normal modes of the mirror in the absence of the black hole. The BQNMs are of course different from the usual quasinormal modes (QNMs) in asymptotically flat spacetimes, because the latter have no mirror and satisfy outgoing wave boundary conditions near spatial infinity, they describe the free oscillations of the black hole spacetime. In the following we shall compute these modes analytically in a certain limit, and numerically by directly integrating the radial equation (6).

B. The black hole bomb: analytical calculation of the unstable modes

In this section, we will compute analytically, within some approximations, the unstable modes of a scalar field in a black hole mirror system. Due to the presence of a reflecting mirror around the black hole, the scalar wave is successively impinging back on the black hole, and amplified.

We assume that $1/\omega \gg M$, i.e., that the Compton wavelength of the scalar particle is much larger than the typical size of the black hole. We will also assume, for simplicity, that $a \ll M$. Following [5, 13], we divide the space outside the event horizon in two regions, namely, the near-region, $r - r_+ \ll 1/\omega$, and the far-region, $r - r_+ \gg M$. We will solve the radial equation (6) in each one of these two regions. Then, we will match the near-region and the far-region solutions in the overlapping region where $M \ll r - r_+ \ll 1/\omega$ is satisfied. Finally, we will insert a mirror around the black hole, and we will find the properties of the unstable modes.

1. Near-region wave equation and solution

In the near-region, $r - r_+ \ll 1/\omega$, the radial wave equation can be written as

$$\Delta \partial_r (\Delta \partial_r R) + r_+^4 (\omega - m\Omega)^2 R - l(l+1)\Delta R = 0. \quad (11)$$

To find the analytical solution of this equation, one first introduces a new radial coordinate,

$$z = \frac{r - r_+}{r - r_-}, \qquad 0 \le z \le 1, \quad (12)$$

with the event horizon being at $z = 0$. Then, one has $\Delta \partial_r = (r_+ - r_-)z\partial_z$, and the near-region radial wave equation can be written as

$$z(1-z)\partial_z^2 R + (1-z)\partial_z R + \varpi^2 \frac{1-z}{z} R - \frac{l(l+1)}{1-z} R = 0, \quad (13)$$

where we have defined the superradiant factor

$$\varpi \equiv (\omega - m\Omega)\frac{r_+^2}{r_+ - r_-}. \quad (14)$$

Through the definition

$$R = z^{i\varpi}(1-z)^{l+1} F, \quad (15)$$

the near-region radial wave equation becomes

$$z(1-z)\partial_z^2 F + \left[(1 + i\,2\varpi) - [1 + 2(l+1) + i\,2\varpi]\,z\right]\partial_z F \\ - \left[(l+1)^2 + i\,2\varpi(l+1)\right] F = 0. \quad (16)$$

This wave equation is a standard hypergeometric equation [14], $z(1-z)\partial_z^2 F + [c - (a+b+1)z]\partial_z F - abF = 0$, with

$$a = l + 1 + i\,2\varpi, \qquad b = l+1, \qquad c = 1 + i\,2\varpi, \quad (17)$$

and its most general solution in the neighborhood of $z = 0$ is $A z^{1-c}F(a-c+1, b-c+1, 2-c, z) + B F(a, b, c, z)$. Using (15), one finds that the most general solution of the near-region equation is

$$R = A z^{-i\varpi}(1-z)^{l+1}F(a-c+1, b-c+1, 2-c, z) \\ + B z^{i\varpi}(1-z)^{l+1}F(a, b, c, z). \quad (18)$$

The first term represents an ingoing wave at the horizon $z = 0$, while the second term represents an outgoing wave at the horizon. We are working at the classical level, so there can be no outgoing flux across the horizon, and thus one sets $B = 0$ in (18). One is now interested in the large r, $z \to 1$, behavior of the ingoing near-region solution. To achieve this aim one uses the $z \to 1 - z$ transformation law for the hypergeometric function [14],

$$F(a-c+1, b-c+1, 2-c, z) = (1-z)^{c-a-b} \\ \times \frac{\Gamma(2-c)\Gamma(a+b-c)}{\Gamma(a-c+1)\Gamma(b-c+1)} F(1-a, 1-b, c-a-b+1, 1-z) \\ + \frac{\Gamma(2-c)\Gamma(c-a-b)}{\Gamma(1-a)\Gamma(1-b)} F(a-c+1, b-c+1, -c+a+b+1, 1-z), \quad (19)$$

and the property $F(a, b, c, 0) = 1$. Finally, noting that when $r \to \infty$ one has $1 - z \to (r_+ - r_-)/r$, one obtains the large r behavior of the ingoing wave solution in the near-region,

$$R \sim A\,\Gamma(1 - i\,2\varpi)\left[\frac{(r_+ - r_-)^{-l}\,\Gamma(2l+1)}{\Gamma(l+1)\Gamma(l+1-i\,2\varpi)} r^l \\ + \frac{(r_+ - r_-)^{l+1}\,\Gamma(-2l-1)}{\Gamma(-l)\Gamma(-l-i\,2\varpi)} r^{-l-1}\right]. \quad (20)$$

2. Far-region wave equation and solution

In the far-region, $r - r_+ \gg M$, the effects induced by the black hole can be neglected ($a \sim 0$, $M \sim 0$, $\Delta \sim r^2$) and the radial wave equation reduces to the wave equation of a massless scalar field of frequency ω and angular momentum l in a flat background,

$$\partial_r^2(rR) + \left[\omega^2 - l(l+1)/r^2\right](rR) = 0. \quad (21)$$

The most general solution of this equation is a linear combination of Bessel functions [14],

$$R = r^{-1/2}\left[\alpha J_{l+1/2}(\omega r) + \beta J_{-l-1/2}(\omega r)\right]. \quad (22)$$

For large r this solution can be written as [14]

$$R \sim \sqrt{\frac{2}{\pi\omega}}\frac{1}{r}\left[\alpha \sin(\omega r - l\pi/2) + \beta \cos(\omega r + l\pi/2)\right], \quad (23)$$

while for small r it reduces to [14]

$$R \sim \alpha \frac{(\omega/2)^{l+1/2}}{\Gamma(l+3/2)}\, r^l + \beta \frac{(\omega/2)^{-l-1/2}}{\Gamma(-l+1/2)}\, r^{-l-1}. \quad (24)$$

3. Matching the near-region and the far-region solutions

When $M \ll r - r_+ \ll 1/\omega$, the near-region solution and the far-region solution overlap, and thus one can match the large r near-region solution (20) with the small r far-region solution (24). This matching yields

$$A = \frac{(r_+ - r_-)^l}{\Gamma(l+3/2)} \frac{\Gamma(l+1)}{\Gamma(2l+1)} \frac{\Gamma(l+1-i\,2\varpi)}{\Gamma(1-i\,2\varpi)} \left(\frac{\omega}{2}\right)^{l+1/2} \alpha, \quad (25)$$

$$\begin{aligned} \frac{\beta}{\alpha} &= \frac{\Gamma(-l+1/2)}{\Gamma(l+3/2)} \frac{\Gamma(l+1)}{\Gamma(2l+1)} \frac{\Gamma(-2l-1)}{\Gamma(-l)} \frac{\Gamma(l+1-i\,2\varpi)}{\Gamma(-l-i\,2\varpi)} \\ &\times \left(\frac{\omega}{2}\right)^{2l+1} (r_+ - r_-)^{2l+1}. \end{aligned} \quad (26)$$

Using the property of the gamma function, $\Gamma(1+x) = x\Gamma(x)$, one can show that $\frac{\Gamma(-l+1/2)}{\Gamma(1/2)} = \frac{(-1)^l 2^l}{(2l-1)!!}$, $\frac{\Gamma(l+3/2)}{\Gamma(1/2)} = \frac{(2l+1)!!}{2^{l+1}}$, $\frac{\Gamma(-2l-1)}{\Gamma(-l)} = \frac{(-1)^{l+1} l!}{(2l+1)!}$ and $\frac{\Gamma(l+1-i\,2\varpi)}{\Gamma(-l-i\,2\varpi)} = i\,(-1)^{l+1} 2\varpi \prod_{k=1}^{l}(k^2+4\varpi^2)$. Then, the matching condition (26) yields

$$\begin{aligned} \frac{\beta}{\alpha} &= i\,2\varpi \frac{(-1)^l}{2l+1} \left(\frac{l!}{(2l-1)!!}\right)^2 \frac{(r_+ - r_-)^{2l+1}}{(2l)!(2l+1)!} \\ &\times \left(\prod_{k=1}^{l}(k^2+4\varpi^2)\right) \omega^{2l+1}. \end{aligned} \quad (27)$$

4. Mirror condition. Properties of the unstable modes

If one puts a mirror near infinity at a radius $r = r_0$, the scalar field must vanish at the mirror surface. Thus, setting the radial field (22) to zero yields the extra condition between the amplitudes α and β, and the position of the mirror r_0,

$$\frac{\beta}{\alpha} = -\frac{J_{l+1/2}(\omega r_0)}{J_{-l-1/2}(\omega r_0)}. \quad (28)$$

This mirror condition together with the matching condition (27) yield a condition between the position of the mirror and the frequency of the scalar wave,

$$\begin{aligned} \frac{J_{l+1/2}(\omega r_0)}{J_{-l-1/2}(\omega r_0)} &= i(-1)^{l+1} \varpi \frac{2}{2l+1} \left(\frac{l!}{(2l-1)!!}\right)^2 \\ &\times \frac{(r_+ - r_-)^{2l+1}}{(2l)!(2l+1)!} \left(\prod_{k=1}^{l}(k^2+4\varpi^2)\right) \omega^{2l+1}. \end{aligned} \quad (29)$$

The solution of (29) can be found in the approximation that applies suitably to this problem, namely, $\omega \ll 1$, and $\mathrm{Re}(\omega) \gg \mathrm{Im}(\omega)$. For very small ω, the r.h.s. of (29) is very small and can be assumed to be zero in the first approximation for ω. This yields

$$J_{l+1/2}(\omega r_0) = 0, \quad (30)$$

which has well studied (real) solutions [14]. We shall label the solutions of (30) as $j_{l+1/2,n}$:

$$J_{l+1/2}(\omega r_0) = 0 \Leftrightarrow \omega r_0 = j_{l+1/2,n}, \quad (31)$$

where n is a non-negative integer number. We now assume that the complete solution to (29) can be written as $\omega \sim j_{l+1/2,n}/r_0 + i\tilde{\delta}/r_0$, where we have inserted a small imaginary part proportional to $\tilde{\delta} \ll 1$. One then has, from (29)

$$\begin{aligned} \frac{J_{l+1/2}(j_{l+1/2,n} + i\tilde{\delta})}{J_{-l-1/2}(j_{l+1/2,n} + i\tilde{\delta})} &= i(-1)^{l+1} \varpi \left(\frac{l!}{(2l-1)!!}\right)^2 \\ &\times \frac{2}{2l+1} \frac{(r_+ - r_-)^{2l+1}}{(2l)!(2l+1)!} \left(\prod_{k=1}^{l}(k^2+4\varpi^2)\right) \omega^{2l+1}. \end{aligned} \quad (32)$$

Now, we can use, for small $\tilde{\delta}$ the Taylor expansion of the l.h.s.,

$$\frac{J_{l+1/2}(j_{l+1/2,n} + i\tilde{\delta})}{J_{-l-1/2}(j_{l+1/2,n} + i\tilde{\delta})} \sim i\,\tilde{\delta} \frac{J'_{l+1/2}(j_{l+1/2,n})}{J_{-l-1/2}(j_{l+1/2,n})} \quad (33)$$

The quantities $j_{l+1/2,n}, J'_{l+1/2}(j_{l+1/2,n}), J_{-l-1/2}(j_{l+1/2,n})$ are tabulated in [14], and can also easily be extracted using Mathematica. Here it is important to note that $J'_{l+1/2}(j_{l+1/2,n})$ and $(-1)^l J_{-l-1/2}(j_{l+1/2,n})$ always have the same sign. Furthermore, for large overtone n, $j_{l+1/2,n} \sim (n+l/2)\pi$. The frequencies of the scalar wave that are allowed by the presence of the mirror located at $r = r_0$ (BQN frequencies) are then

$$\omega_{BQN} \simeq \frac{j_{l+1/2,n}}{r_0} + i\delta, \quad (34)$$

where n is a non-negative integer number, labelling the mode overtone number. For example, the fundamental mode corresponds to $n = 0$. In (34), $\delta = \mathrm{Im}[\omega_{BQN}]$ is obtained by substituting (33) in (32),

$$\delta \simeq -\gamma \frac{(-1)^l J_{-l-1/2}(j_{l+1/2,n})}{J'_{l+1/2}(j_{l+1/2,n})} \frac{j_{l+1/2,n}/r_0 - m\Omega}{r_0^{2(l+1)}}, \quad (35)$$

where

$$\begin{aligned} \gamma &\equiv \left(\frac{l!}{(2l-1)!!}\right)^2 \frac{r_+^2 (r_+ - r_-)^{2l}}{(2l)!(2l+1)!} \\ &\times \frac{2}{2l+1} \left(\prod_{k=1}^{l}(k^2+4\varpi^2)\right) [j_{l+1/2,n}]^{2l+1}. \end{aligned} \quad (36)$$

Notice that δ is very small for large r_0 and thus satisfies the conditions that go with the approximation used, $\mathrm{Re}(\omega) \gg \mathrm{Im}(\omega)$. Equations (34) and (35) constitute the main results of this section. Two important features of this system, black hole plus mirror, can already be read from the equations above: first, from equations (34) and (35) one has,

$$\delta \propto -(\mathrm{Re}[\omega_{BQN}] - m\Omega). \tag{37}$$

Therefore, $\delta > 0$ for $\mathrm{Re}[\omega_{BQN}] < m\Omega$, and $\delta < 0$ for $\mathrm{Re}[\omega_{BQN}] > m\Omega$. The scalar field Φ has the time dependence $e^{-i\omega t} = e^{-i\mathrm{Re}(\omega)t}e^{\delta t}$, which implies that for $\mathrm{Re}[\omega_{BQN}] < m\Omega$, the amplitude of the field grows exponentially and the BQNM becomes unstable, with a growth timescale given by $\tau = 1/\delta$. In this case, we see that the system behaves in fact as a bomb, a black hole bomb. Second,

$$\mathrm{Re}[\omega_{BQN}] = \frac{j_{l+1/2,n}}{r_0}, \tag{38}$$

showing that the wave frequency is proportional to the inverse of the mirror's radius. As one decreases the distance at which the mirror is located, the allowed wave frequency increases, and there will thus be a critical radius at which the BQN frequency no longer satisfies the superradiant condition (10). Notice also that $\mathrm{Re}[\omega_{BQN}]$ as given by (38) is equal to the normal mode frequencies of a spherical mirror in a flat spacetime [15]. In the next subsection, when the numerical results will also be available, we will return to this discussion.

C. The black hole bomb. Numerical approach

1. Numerical procedure

In the numerical calculation for determining oscillation frequencies of the modes, we use the same function as that defined by Teukolsky [16] given by (see also [17])

$$Y = (r^2 + a^2)^{1/2}R. \tag{39}$$

Then, Teukolsky equation becomes a canonical equation, given by

$$\frac{d^2}{dr_*^2}Y + VY = 0, \tag{40}$$

where

$$V = \frac{K^2 - \lambda\Delta}{(r^2 + a^2)^2} - G^2 - \frac{d}{dr_*}G, \tag{41}$$

with $K = (r^2 + a^2)\omega - am$, and $G = r\Delta(r^2 + a^2)^{-2}$. For the separation constant $\lambda = A_{lm} + a^2\omega^2 - 2am\omega$, we make use of a well known series expansion in $a\omega$, given by

$$\lambda = a^2\omega^2 - 2am\omega + \sum_{i=0}^{\infty} {}_0f_i^{lm}(a\omega)^i, \tag{42}$$

where ${}_0f_i^{lm}$ is the expansion coefficient (for the explicit form, see, e.g., [12]). In this study, we keep the terms in the expansion up to an order of $(a\omega)^2$. As mentioned, near the horizon, the physically acceptable solution of equation (40) is the incoming wave solution, given by

$$Y = e^{-i(\omega-m\Omega)r_*}[y_0 + y_1(r - r_+) + y_2(r - r_+)^2 + \cdots] \tag{43}$$

where y_i is the expansion coefficient determined by ω and y_0. Here, we do not show explicit expression for the y_i's because it is straightforward to derive it.

In order to obtain the proper solutions numerically, by using a Runge-Kutta method, we start integrating the differential equation (40) outward from $r = r_+(1 + 10^{-5})$ with the asymptotic solution (43). We then stop the integration at the radius of the mirror, $r = r_0$, and get the value of the wave function at $r = r_0$, which is considered a function of the frequency, $Y(r_0, \omega)$. If $Y(r_0, \omega) = 0$, the solution satisfies the boundary condition of perfect reflection due to the mirror and the frequency ω is a BQN frequency, which we label as ω_{BQN}. In other words, the dispersion relation of our problem is given by the equation $Y(r_0, \omega_{BQN}) = 0$. In order to solve the algebraic equation $Y(r_0, \omega_{BQN}) = 0$ iteratively, we use a secant method. Here, it is important to note that if the mode is stable or $\mathrm{Im}(\omega_{BQN}) < 0$, the asymptotic solution (43) diverges exponentially and another independent solution, which is unphysical, damps exponentially as $r_* \to -\infty$.

2. Numerical results

Our numerical results are summarized in Figs. 1-7. As we remarked earlier, we only show the data corresponding to the unstable BQNMs. We have also found the stable modes, but since they lead to no bomb we refrain from presenting them. ¿From the figures we confirm the analytical expectations. In addition we can discuss growing timescales, oscillation frequencies, energy extracted and efficiencies with great accuracy. Figure 1 plots the imaginary part of the BQN frequency for the fundamental BQNM as a function of the mirror's location r_0 and the rotation parameter a. In figure 2, we show the real part of the BQN frequency for the fundamental BQNM also as a function of r_0 and a. Supporting the analytical results, figure 1 shows that: (i) The instability is weaker (the growing timescale $\tau = \frac{1}{\mathrm{Im}[\omega_{BQN}]}$ is larger) for larger mirror radius, meaning that $\mathrm{Im}[\omega_{BQN}]$ decreases as r_0 increases. This is also expected on physical grounds, as was remarked in [7], if one views the process as one of successive amplifications and reflections on the mirror. (ii) As one decreases r_0 the instability gets stronger, as expected, but surprisingly, suddenly the BQNM is no longer unstable. The imaginary component of ω_{BQN} drops from its maximum value to zero, and the mode becomes stable at a critical radius r_0^{crit}. Physically, this happens because superradiance generates wavelengths with $\lambda > 1/\Omega$. So the mirror at a distance r_0 will "see" these wavelengths
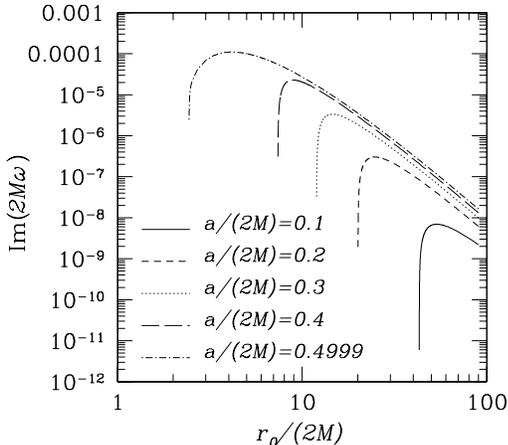
FIG. 1: The imaginary part of the fundamental ($n = 0$) BQN frequency (ω_{BQN}) as a function of the mirror's location r_0 is plotted. The plot refers to a $l = m = 1$ wave. It is also shown the dependence on the rotation parameter a. One sees that for r_0 greater than a critical value, r_0^{crit}, depending on a, there is the possibility of building a bomb. Moreover, the imaginary component of the BQN frequency decreases abruptly from its maximum value to zero at r_0^{crit}. For $r_0 < r_0^{\text{crit}}$ the BQNM is stable. Tracking the mode to yet smaller distances shows that indeed it remains stable (the imaginary part of ω_{BQN} is negative).

if $r_0 > r_0^{\text{crit}} \sim \lambda \sim 1/\Omega$. One can improve the estimate for r_0^{crit} using equations (10), (37), and (38), yielding $r_0^{\text{crit}} \sim \frac{j_{l+1/2,n}}{m\Omega}$. This estimate for the critical radius matches very well with our numerical data, even though the analytical calculation is a large wavelength approximation. In fact, to a great accuracy r_0^{crit} is given by the root of $\text{Re}[\omega(r_0^{\text{crit}})] - m\Omega = 0$, as is shown in figure 3. Also supporting the analytical results, figure 2 shows that $\text{Re}[\omega_{BQN}]$ behaves as $\frac{1}{r_0}$, which is consistent with equation (34). This means that it is indeed the mirror which selects the allowed vibrating frequencies. The results for higher mode number n is shown in figures 4 and 5, and the behaviour agrees with the picture provided by the analytical approximation. The agreement between the analytical and numerical results is best seen in Table I, where we show the lowest BQN frequencies obtained using both methods. In figures 6 and 7 we show the numerical results referring to different values of the angular number l and m. Our numerical results indicate that $\frac{1}{\text{Im}[\omega_{BQN}]} \sim r_0^{-2(l+1)}$, in agreement with the analytical result, equation (35). The numerical results also indicate that the oscillating frequencies ($\text{Re}[\omega_{BQN}]$) scale with l, more precisely, $\text{Re}[\omega_{BQN}]$ behaves as $\text{Re}[\omega_{BQN}] \sim \pi/r_0(n + l/2)$. This behavior is also predicted by the analytical study.
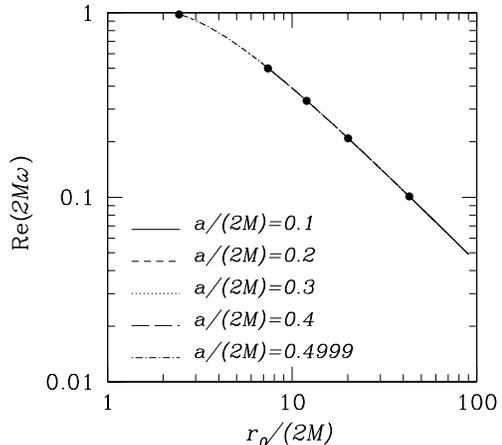
FIG. 2: The real part of the fundamental ($n = 0$) BQN frequency (ω_{BQN}) as a function of the mirror's location r_0 is plotted. The plot refers to a $l = m = 1$ wave. There is no perceptive a-dependence (as matter of fact there is a very small a-dependence but too small to be noticeable). Thus, the oscillation frequency basically depends only on r_0, and for large r_0 goes as $1/r_0$, as predicted by the analytical formula (34). The dots indicate r_0^{crit} (cf. Fig. 1).

TABLE I: The fundamental BQN frequencies for a black hole with $a = 0.8M$ and a mirror placed at $r_0 = 100M$. The data corresponds to the $l = m$ modes, and the frequency is measured in units of the mass M of the black hole. We present both the numerical (ω_{BQN}^N) and analytical (ω_{BQN}^A) results. Notice that the agreement between the two is very good, and it gets better as l increases. Also, we have checked that for very large r_0 the two yield basically the same results.

$a = 0.8M$, $r_0 = 100M$		
l	ω_{BQN}^N:	ω_{BQN}^A:
1	$8.75 \times 10^{-2} + 1.19 \times 10^{-7}i$	$8.99 \times 10^{-2} + 1.41 \times 10^{-7}i$
2	$1.13 \times 10^{-1} + 6.77 \times 10^{-12}i$	$1.15 \times 10^{-1} + 6.89 \times 10^{-12}i$
3	$1.37 \times 10^{-1} + 2.45 \times 10^{-16}i$	$1.39 \times 10^{-1} + 2.26 \times 10^{-16}i$

Let us now take Press and Teukolsky example of a black hole with mass $M = 1M_\odot$ [7]. We are now in a position to make a much improved quantitative analysis. We take $a = 0.8\,M$, a large angular momentum so that we make a full use of our results. In addition, to better take advantage of the whole process, one should place the mirror at a position near the point of maximum growing rate, but farther. Thus, for the example, $r_0 \sim 22M \sim 33\,\text{Km}$ (see Fig. 1). This gives a growing timescale of about $\tau \sim 0.6\,\text{s}$ (see also Fig. 1), which means that every 0.6 s the amplitude of the field gets approximately doubled. This means that at the end of 13 seconds the initial amplitude of the wave has grown to 10^7 of its initial value, and that thus the energy content is 10^{14} times greater than the initial perturbation. We con-
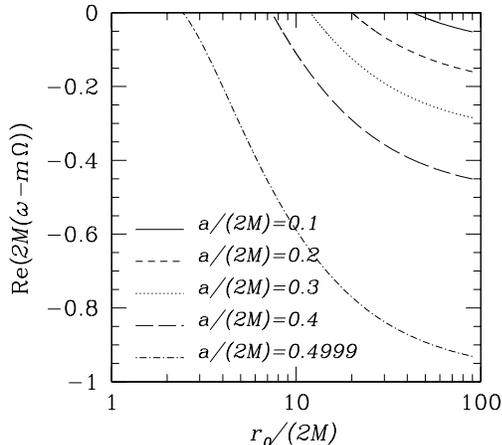
FIG. 3: This figure helps in understanding why the instability disappears for r_0 smaller than a certain critical value. The condition for superradiance is $\omega - m\Omega < 0$. Since ω goes as $1/r_0$ (check Fig. 2), then it is expected that the condition will stop to hold at a critical r_0. This is clearly seen here. Note that the critical value of r_0 is in excellent agreement with that shown in Fig. 1.

FIG. 5: Same as Fig. 4, but for the real part of ω_{BQN}.

FIG. 4: The imaginary part of the BQN frequency as a function of r_0, for $a = 0.4$ and for the three lowest overtones n, for $l = m = 1$. As expected from the general arguments presented, higher overtones get stable at larger distances, and attain a smaller maximum growing rate.
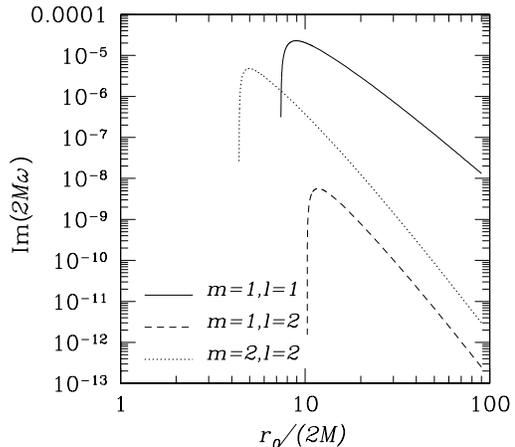
FIG. 6: The imaginary part of the fundamental ω_{BQN} for an $a = 0.4$ black hole, as a function of the mirror's location r_0 here shown for some values of l, m. Furthermore, as is evident from this figure and also as could be anticipated, the larger m the smaller r_0 can be, still displaying instability. Note however that the maximum instability is larger for the $m = 1$ mode. This is a general feature. The imaginary part of the frequency seems to behave as $\mathrm{Im}[\omega_{BQN}] \sim r_0^{-2(l+1)}$, which agrees with the analytical prediction (35).

sider there are no losses through the mirror and assume the process to be adiabatic. Using the first law of thermodynamics one can then set $\Delta M \sim \Omega \Delta J$, where ΔM and ΔJ are the changes in mass and angular momentum of the black hole in this process, respectively. Now, the black hole is losing angular momentum in each superradiant scattering. Thus a decreases. If we go to figure 1

we see that r_0^{crit} increases with decreasing a. At a certain stage r_0^{crit} coincides with the position of the mirror at r_0, at which point there is no more possibility of superradiance. The process is finished. Thus from figure 1, or more accurately from our numerics, one can find Δa, and thus ΔJ. Then ΔM follows from $\Delta M \sim \Omega \Delta J$. In the example this gives a total amount $\Delta M \sim 0.01M$ of extracted energy before the bomb stops functioning. The process has thus an efficiency of 1%, about the same
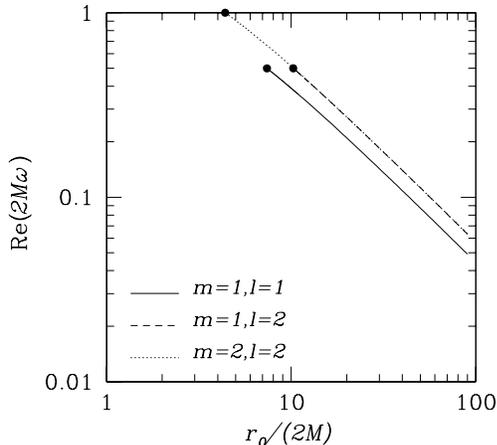
FIG. 7: Same as Fig. 6 but for the real part. Note that there is an l-dependence of the real part of the frequency. On the other hand, there is no noticeable m-dependence, in accordance with the analytical result (34).

order of magnitude as the efficiency of nuclear fusion of hydrogen burning into helium ($\sim 0.7\%$). If, instead, the mirror is placed at $r_0 \sim 200M \sim 300$Km one still gets a good growing timescale of about 15 min. This means that at the end of 6 hours the initial amplitude of the wave has grown to 10^7 of its initial value. In this case $\Delta M \sim 0.1\,M$, with a 10% efficiency, and one can show that the efficiency grows with mirror radius r_0. Since the cost of mirror construction scales as r_0^2, we see that small mirrors are more effective. One can give other interesting examples. For a black hole at the center of a galaxy, with mass $M \sim 10^8 M_\odot$, $a = 0.8M$, and $r_0 = 22\,M$, the maximum growing timescale is of the order of 2 years. Another interesting situation happens when the black hole has a mass of the order of the Earth mass. In this case, by placing the mirror at $r_0 = 1\,$m one gets a growing timescale of about $0.02\,$s. At the other end of the black hole spectrum one can consider Planck size black holes.

D. Zel'dovich's cylinder surrounded by a mirror

As a corollary, we discuss here electromagnetic superradiance in the presence of a cylindrical rotating body, a situation first discussed by Zel'dovich [3]. He noted that by surrounding this rotating body with a reflecting mirror one could amplify the radiation, much as the black hole bomb process just described. Bekenstein and Schiffer [19] have recently elaborated on this. An independent analytical approximation, similar in all respects to the one we discussed earlier in the black hole bomb context, can also be applied here for finding the BQN frequencies of this system (conducting cylinder plus reflecting mirror), and leads to almost the same results as

for the black hole bomb. The imaginary component of ω_{BQN} is $\delta \propto -(\mathrm{Re}[\omega_{BQN}] - m\Omega)$. The electromagnetic field has the time dependence $e^{-i\omega t} = e^{-i\mathrm{Re}(\omega)t}e^{\delta t}$ and thus, for $\mathrm{Re}[\omega_{BQN}] < m\Omega$, the amplitude of the field grows exponentially with time and the mode becomes unstable, with a growth timescale given by $\tau = 1/\delta$. Second, $\mathrm{Re}[\omega_{BQN}] \propto 1/r_0$, i.e., the wave frequency is proportional to the inverse of the mirror's radius, as it was for the black hole bomb. Therefore, as one decreases the distance at which the mirror is located, the allowed wave frequency increases, and again there will be a critical radius at which the frequency no longer satisfies the superradiant condition (10). If one tries to use the system as it is, it would be almost impossible to observe superradiance in the laboratory. Take as an example a cylinder with a radius $R = 10\,$cm, rotating at a frequency $\Omega = 2\pi \times 10^2\,\mathrm{s}^{-1}$, and a surrounding mirror with radius $r_0 = 20\,$cm. For the system to be unstable and experimentally detectable, the minimum mirror radius is given by $r_{\mathrm{crit}} \sim \frac{c}{m\Omega}$ (where we have reinstated the velocity of light c), which yields $r_{\mathrm{crit}} \sim 1000\,$Km, for a $m = 1$ wave. It seems impossible to use this apparatus to measure superradiance experimentally. A way out of this problem may be the one suggested in [19]: to surround the conducting mirror by a material with a low velocity of light. In this case the critical radius would certainly decrease, although further investigation is needed in order to ascertain what kind of material should be used.

III. ARE KERR-ADS BLACK HOLES UNSTABLE?

A spacetime with a naturally incorporated mirror in it is anti-de Sitter (AdS) spacetime, which has attracted a great deal of attention recently due to the AdS/CFT correspondence and other matters. As is well known, anti-de Sitter (AdS) space behaves effectively as a box, in other words, the AdS infinity works as a mirror wall. Thus, one might worry that Kerr-AdS black holes could behave as the black hole bomb just described, and that they would be unstable. Hawking and Reall [10] have shown that, at least for large Kerr-AdS black holes, this instability is not present. The stability of large Kerr-AdS black holes in four and higher dimensions can be understood in yet another way, using the knowledge one acquired from the black hole bomb study. The black hole rotation is constrained to be $a < \ell$, where ℓ is the AdS radius [10]. Large black holes are the ones for which $r_+ >> \ell$. In this case the angular velocity of the horizon $\Omega = \frac{a}{r_+^2 + a^2}(1 - a^2/\ell^2)$ goes to zero and one expects that the rotation plays a neglecting role in this regime, with the results found for the non-rotating AdS black hole [20, 21] still holding approximately when the rotation is non-zero. The characteristic quasinormal frequencies for large, non-rotating AdS black holes were computed in [20, 21] showing that the real part scales with r_+. Now, since $\Omega \to 0$ for large black holes and the QNMs have a

very large real part, one can understand why there is no instability: superradiant modes are simply not excited, as the condition for superradiance, $\omega < m\Omega$, cannot be fulfilled. We could try to evade this by going to higher values of m, but then l has also to be large ($l \geq m$). However, for large l's, the real part of the QNMs is known to scale with l [22], thus the condition for superradiance is never fulfilled. What about small Kerr-AdS black holes, $r_+ << \ell$? Considering the case a small, $a << r_+$ say, is enough for our purposes. In this situation the horizon's angular velocity scales as the inverse of r_+, and it can be made arbitrarily large. Although the effect of rotation cannot be neglected in this case, the results of the QNM analysis for non-rotating AdS black holes give some hints on what may happen. For small non-rotating AdS black holes, the QN frequencies have a real part that goes to a constant, independent of r_+, whereas the imaginary part goes to zero [21]. If we add a small angular momentum per unit mass a to the black hole, we do not expect the real part of the QN frequency to grow significantly. But, since Ω is very large anyway, the superradiance condition $\omega < m\Omega$ will most likely be fulfilled. Therefore we expect to be possible to excite the superradiant instability in these spacetimes.

IV. CONCLUSIONS

To conclude, we have investigated the black hole bomb thoroughly, by analytical means in the long wavelength limit, and numerically. We have provided both analytical and numerical accurate estimates for growing timescales and oscillation frequencies of the corresponding unstable Boxed Quasinormal Modes (BQNMs). Both results agree and yield consistent answers. An important feature born out in this work is that there is a minimum distance at which the mirror must be located in order for the system to become unstable and for the bomb to work. Basically this is because the mirror selects the frequencies that may be excited. For distances smaller than this, the system is stable and the perturbation dies off exponentially. This minimum distance increases as the rotation parameter decreases. We have given an explicit example where such a system works yielding a reliable source of energy. By using appropriately this extracted energy one could perhaps build a black hole power plant. Although we have worked only with zero spin (scalar) waves, we expect that the general features for other spins will be the same. Moreover, it is known that a charged black hole, even in the absence of rotation, provides a background for superradiance, as long as the impinging wave is a bosonic charged wave (fermions do not exhibit superradiance). In this case, the critical radius should be of order $r_{\mathrm{crit}} \sim \frac{1}{e\Phi}$, where e is the charge of the scalar particle and Φ is the black hole's electromagnetic potential.

We have also shown that a mirror surrounding Zel'dovich's rotating cylinder leads to a system that dis-

plays the same instabilities as the black hole bomb. However, for the instability to be triggered in an Earth based experiment, some improvments must be made. In particular the cylinder should be surrounded by a material with a low light velocity, since otherwise it would require huge mirror radius or huge rotating frequencies.

The study of the black hole bomb, and of the associated instabilities allows one to better understand the absence of superradiance in large Kerr-AdS black holes [10] and moreover to expect that small Kerr-AdS black holes will be unstable.

Finally, it seems worth investigating whether or not this kind of black hole bomb is possible in TeV-scale gravity. In these scenarios, one has four non-compact dimensions and n extra compact dimensions. It might be possible that these extra compactified dimensions work as a reflecting mirror, and therefore rotating black holes in $4 + n$ dimensions could turn out to be unstable.

We would also like to make a remark on a possible astrophysical application of this black hole-reflecting wall system. It has been proposed in [23], and further discussed in [24], that the superradiant amplification process might provide the energy necessary to feed the highly energetic gamma-ray burst. Magnetosonic plasma waves, generated in the accreting plasma around an astrophysical black hole, might enter in the waveguide cavity located between the gravitational potential barrier of the black hole and the inner edge of the accretion disk. Once there, the inner boundary of the accretion disk might act as a reflecting wall, and waves can then suffer multiple reflection and superradiant amplification, increasing their energy. This energy increase will continue until the magnetosphere that surrounds the system is no longer capable of supporting the energy pressure in the waveguide cavity. The wave energy would then be released in a burst, and collimated into a relativistic jet by, e.g., the Blandford-Znajek process [25], and finally transferred into the observed γ-ray photons, as described by the Fireball model [26]. In order to better compare the energy and timescales derived from the superradiant model with the observational data taken from gamma-ray bursts, it is appropriate to apply the methods of this paper to superradiant cavities that have an accreting matter configuration of a torus or disk.

36280/99.

[1] For a very good review on the subject as well as a careful explanation of various misinterpretations that have appeared over the years concerning the Klein paradox, we refer the reader to: C. A. Manogue, Annals of Physics **181**, 261 (1988).

[2] W. Greiner, B. Müller and J. Rafelski, *Quantum electrodynamics of strong fields*, (Springer-Verlag, Berlin, 1985).

[3] Ya. B. Zel'dovich, Pis'ma Zh. Eksp. Teor. Fiz. **14**, 270 (1971) [JETP Lett. **14**, 180 (1971)]; Zh. Eksp. Teor. Fiz **62**, 2076 (1972) [Sov. Phys. JETP **35**, 1085 (1972)].

[4] J. M. Bardeen, W. H. Press and S. A. Teukolsky, Astrophys. J. **178**, 347 (1972).

[5] A. A. Starobinsky, Zh. Eksp. Teor. Fiz **64**, 48 (1973) [Sov. Phys. JETP **37**, 28 (1973)]; A. A. Starobinsky and S. M. Churilov, Zh. Eksp. Teor. Fiz **65**, 3 (1973) [Sov. Phys. JETP **38**, 1 (1973)].

[6] S. A. Teukolsky and W. H. Press, Astrophys. J. **193**, 443 (1974).

[7] W. H. Press and S. A. Teukolsky, Nature **238**, 211 (1972).

[8] T. Damour, N. Deruelle and R. Ruffini, Lett. Nuovo Cimento **15**, 257 (1976).

[9] S. Detweiler, Phys. Rev. D **22**, 2323 (1980); T. M. Zouros and D. M. Eardley, Annals of Physics **118**, 139 (1979); H. Furuhashi and Y. Nambu, gr-qc/0402037.

[10] S. W. Hawking and H. S. Reall, Phys. Rev. D **61**, 024014 (1999).

[11] D. R. Brill, P. L. Chrzanowski, C. M. Pereira, E. D. Fackerell and J. R. Ipser, Phys. Rev. D **5**, 1913 (1972); S. A. Teukolsky, Phys. Rev. Lett **29**, 1114 (1972).

[12] E. Seidel, Class. Quantum Grav. **6**, 1057 (1989).

[13] W. G. Unruh, Phys. Rev. D **14**, 3251 (1976).

[14] M. Abramowitz and A. Stegun, *Handbook of mathematical functions*, (Dover Publications, New York, 1970).

[15] L. Landau and E. Lifshitz, *Quantum mechanics, nonrelativistic theory* (Mir, Moscow, 1974).

[16] S.A. Teukolsky, Astrophys. J. **185**, 635 (1973).

[17] S. A. Hughes, Phys. Rev. D **62**, 044029 (2000); Erratum-ibid. D **67**, 089902 (2003).

[18] E. W. Leaver, Proc. R. Soc. London A**402**, 285 (1985).

[19] J. D. Bekenstein and M. Schiffer, Phys. Rev. D **58**, 064014 (1998).

[20] G. T. Horowitz, and V. Hubeny, Phys. Rev. D **62**, 024027(2000); V. Cardoso and J. P. S. Lemos, Phys. Rev. D **64**, 084017 (2001); E. Berti, K. D. Kokkotas, Phys. Rev. D **67**, 064020 (2003).

[21] V. Cardoso, R. Konoplya, J. P. S. Lemos, Phys. Rev. D **68**, 044024 (2003).

[22] V. Cardoso, unpublished.

[23] M. H. P. M. Putten, Science **284**, 115 (1999).

[24] A. Aguirre, Astrophys. J. **529**, L9 (2000).

[25] R. D. Blandford and R. L. Znajek, Mon. Not. Roy. Astron. Soc. **179**, 433 (1997).

[26] T. Piran, Phys. Rep. **314**, 575 (1999); P. Mészáros, Ann. Rev. of Astron. and Astrophys. **40**, 137 (2002).